PNCT841-79-37

Friction Coefficient Measurements and Analysis of Local Stress/Strain in Zircaloy-2 Cladding

T. TACHIBANA

N. NAKAE

H. KANEKO

Y. HONDA

Plutonium Fuel Division, Tokai Works,

Power Reactor and Nuclear Fuel Development Corporation

Tokai-mura, Ibaraki-ken, 319-11, Japan

For Presentation at

THE ENLARGED HALDEN PROGRAMME GROUP MEETING

ON

Fuel Performance Experiment and Evaluation

- Hankö Fjordhotell, 17th-21st June, 1979 -

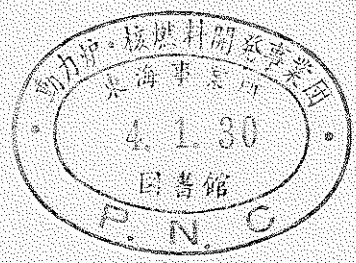

Friction Coefficient Measurements and Analysis of Local Stress/Strain in Zircaloy-2 Cladding

T. TACHIBANA, N. NAKAE, H. KANEKO and Y. HONDA

Plutonium Fuel Division, Tokai Works,
Power Reactor and Nuclear Fuel Development Corporation,
Tokai-mura, Ibaraki-ken, 319-11, Japan

Abstract

In the present study, the friction coefficient between UO_2 pellet and Zry-2 cladding was successfully measured by out-of-pile experiments. The friction coefficient under a condition of hard contact was about 0.5 at temperature region of 300-400 ^{o}C. Using the results, calculation was performed to obtain the local stress/strain distributions in Zry-2 cladding when a radially cracked pellet expanded outwardly after contact with the cladding. The calculation was carried out by finite element code in which a system of friction between pellet and cladding was introduced. Local strain concentrations appeared not only at the position just facing pellet's crack but also at the position apart from the cracks when the friction coefficient became larger than 1.0. From the analysis it was concluded that keeping the friction coefficient below 0.5 in fuel rod must be one of measures which prevent PCI-induced SCC failure.

CONTENTS

1. Introduction

Crackings of fuel pellets are induced by the difference of thermal expansions during reactor operation. As a result of the fuel cracking, fuel fragments move outward the inner surface of cladding. A hard contact between fuel and cladding is expected to occur due to the fuel relocation together with thermal expansion and fuel swelling. It has been reported that a local stress and strain occurred at the inner surface of cladding faced to the cracks [1]. A failure of cladding usually initiated at a position where peak and/or maximum stress and strain appeared. It is considered that the failure occurs as a result of stress corrosion cracking (SCC) and is accelerated by the hard contact between pellet and cladding (PCI). For predicting the failure due to PCI accompanied with SCC, it is most important to evaluate the maximum stress and strain occurred at the inner surface of cladding. Gittus et al. [2,3] introduced theoretically the equation representing the strain concentration factor (α) as follows; $\alpha = 2\pi\mu/mN$, where N is the number of cracks, μ the friction coefficient between pellet and cladding, and m the modulus of strain-hardening. They treated only the closed cracks and did not considered the effects of geometrical feature of cracks and the contact force between pellet and cladding on the factor (α).

In the resent paper, circumferential distributions of stress, strain and strain concentration factor at the inner surface of cladding were analysed by means of the finite element method using the PLASTIC code. The code can treat two dimensional (R-θ) problem and the phenomena of frictional sliding between pellet and cladding. The friction coefficients of UO_2/Zry-2 were not previously measured under a high contact load. The friction coefficients were successfully measured between UO_2 pellet and Zry-2 cladding under a high contact load. The results were used in the above calculations. The result of the calculations will be very helpful to predict the cladding failure due to PCI during reactor operation.

One object of this study is to know the behavior of stress

and strain in claddings under the friction phenomena, and also to find out the best way for preventing the cladding failure due to PCI.

2. Out-of-pile measurements of friction coefficient between UO_2 pellet and Zry-2 cladding

2-1 Specimens

UO_2 pellets having 94 $\pm$ 1 % of theoretical density were obtained by sintering in the mixture gas of H_2 and N_2 (3 : 1) and the dimension was 13.6 mm in diameter and 20.0 mm in height. Commercially available Zry-2 cladding (O.D. = 16.5 mm and I.D. = 14.7 mm) was cut into semi-circular form and used in this study. Both the pellet and cladding specimen were fixed on jigs of heat resistant steel for the friction test. Fig. 1 shows a configuration of the pellet and cladding specimen.

2-2 Apparatus and testing procedure

An apparatus for the friction coefficient measurements is consisted with two sets of Instron-type compression device. One of them applies a controlled vertical contact load (F_n) on the pellet and cladding specimen, and the other gives a horizontal sliding force (F_s) to the cladding specimen. This apparatus is equipped with a floating unit on the upper section of the vertical compression device, and the floating unit is supported by oil pressure. Due to this floating unit the vertical compression device can move freely by the horizontal sliding force. It is, therefore, considered that the effect of the compression device on the detected sliding force (F_s) is negligibly small. Fig. 2 shows a sketch of the apparatus , and Fig. 3 shows a typical sliding behavior for UO_2 pellet and Zry-2 cladding specimen.

Static and dynamic coefficients of friction (these were denoted by μ_s and μ_D, respectively) were obtained by the usual manner based on the definition of friction coefficient as follows;

for the static coefficient of friction,

$$\mu_s = {}^{s}F_s / F_n \quad , \tag{1}$$

and for the dynamic coefficient of friction,

$$\mu_D = {}^{D}F_s / F_n \quad , \tag{1'}$$

where F_s and F_n are the detected sliding and contact forces, respectively, and the suffixes of s and D mean static and dynamic.

Measurements were carried out at temperatures up to 400 ^{o}C in a highly purified helium gas flow. The friction coefficients were measured on three or four sets of specimens at each temperature.

2-3 Results of friction coefficient measurements

Both the static and dynamic coefficient of friction are almost the same in the temperature range examined at typically shown in Fig. 3. The friction coefficients between UO_2 pellet and Zry-2 cladding are shown in Fig. 4. The coefficient is 0.32 $\pm$ 0.09 at room temperature and 0.48 $\pm$ 0.09 at 400 ^{o}C. The gradual increase of the coefficients is observed in the temperature range up to 400 ^{o}C. The results obtained in this measurements were used in the following PCI analysis.

3. Analysis of local stress/strain in Zry-2 cladding

3-1 Model for local stress/strain analysis

Local stress and strain in Zry-2 cladding due to expansion of radially cracked fuel pellets are evaluated in this section by use of the finite element method. A plane stress model used in this analysis is shown in fig. 5. In the model, the fuel pellet is divided into two regions, outer and inner, at one third of the radius. The outer region of the pellet is assumed to be sepa-

rated into eight fragments by eight radial cracks with 45 ^{o} of the crack angle at the tips. The inner region is assumed to work as a source of a hydrostatic pressure to press the fuel fragments outwardly. As shown in the figure, a friction layer which is a very thin fictitious layer of 20 μm thickness is introduced at pellet/cladding interface. The layout of finite elements is shown in Fig. 6. Half of the pellet fragment is divided into 78 elements and the corresponding cladding into 89 elements. The fictitious layer is divided radially into 28 regions and each region is further divided into four elements.

3-2 Description of the PLASTIC code

The PLASTIC code has been developed to calculate stress/strain distribution from viewpoint of mechanics and makes it possible to perform two-dimensional elastic-plastic analysis including a slipping phenomenon. Direct interation method [4] based on the yield criterion of Von Mises is adopted in the PLASTIC code in order to take into account the phenomenon that a symmetric slippage occurs at the interface between cladding and pellet with symmetric distribution of cracks (see Fig. 5). A following special system is incorporated into the PLASTIC code. Plastic flows arise in the fictitious thin layer when the stress ratio, σ_p(peripheral stress) / σ_R(radial stress) exceeds the friction coefficient, μ(a setting value), and local slippages continue until the stress ratio becomes smaller than μ.

The flow diagram for the PLASTIC is given in Fig. 7, and the detailed procedure in the calculation is listed below;

1] At first the fictitious layer of pellet/cladding interface is assumed, if not slip.
2] Stiffness matrix for each element is calculated.
3] Stiffness matrixes are incorporated into the entire coordinate.
4] Displacements of nodal points are calculated from all stiffness matrixes and external forces.
5] The stresses in X-direction, σ_X, those in Y-direction, σ_Y, and the shear stresses are calculated from displacements and stress matrixes.

6] The principal stresses, σ_1 and σ_2, and the angles, θ, of the principal stresses are calculated.

7] The equivalent stress, σ_e, is calculated by means of the Von Mises's equation from σ_1 and σ_2 for each element.

8] Each element is judged to be yielded when $\sigma_e \geqq \sigma_y$, and not to be yielded when $\sigma_e < \sigma_y$, where σ_y is the yield strength of the material.

9] If an element is decided to be yielded, the plastic constant (M) is calculated from the linearity of the stress-strain curve for the material and the above calculations are made again from the first using the plastic constant instead of the elastic constant (E).

10] The calculations by use of the new plastic constant are repeated until the ratio of σ_e for the yielded element to the stress obtained by the stress-strain curve becomes larger than 0.999.

11] Next, the friction phenomenon is considered.

12] The region in the friction layer is permitted to cause a plastic flow, when the ratio of σ_p/σ_R is larger than μ for each region. In this case, the yield strength of the elements included in the region is modified to be a lower value than σ_e.

13] Such as operation as mentioned above is repeated, until the value of σ_p/σ_R for each element concerned becomes smaller than μ.

14] A series of calculations is completed, if the ratios of σ_g to σ in the stress-strain curve become 0.999-1.000 for all elements and the values of σ_p/σ_R become smaller than μ for the elements in the layer.

The values of mechanical properties used in this calculation are summarized in Table 1.

3-3 Results of the local stress/strain analysis

In order to analyse the pellet and cladding mechanical interaction by use of the PLASTIC, normal pressure were applied on a pellet from it's center instead of the expansion of pellet [6], and it was said that the procedure could simulate the mechanically

applied load condition of cladding [7]. The friction coefficients between pellet and cladding are selected to be 0.5, 1.0 and 1.5 for the reason mentioned in the preceeding section (2-3).
The maximum stress and strain are plotted in Figs. 8 and 9, respectively. The maximum hoop strain at $\mu = 0.5$ is almost constant in the range up to 0.75 % of the fractional displacement of cracked pellet. A strain concentration factor, α, in a cladding was defined as follows;

$$\alpha = \varepsilon_{\theta max} / \bar{\varepsilon}_{\theta}, \qquad (2)$$

where $\varepsilon_{\theta max}$ is a maximum circumferential strain and $\bar{\varepsilon}_{\theta}$ a mean circumferential strain in cladding.
The maximum concentration factor, α, is plotted as a function of the fractional changes of radial displacement of pellet in Fig. 10. The strain concentration factor remains to be constant in the range where the cladding is deformed in elastic, and it increases with increasing the radial displacement in the plastic deformation region. The slope becomes steep in the case that μ is more than 1.0.

The strain distribution in the inner surface of cladding is shown in Fig. 11. It is found that when μ gets larger, the circumferential strain and also stress become higher in the vicinity of the pellet's cracks. The highest strain induced by PCI occurs at the inner surface of cladding faced to the pellet's cracks in most cases, and it tends to be smaller in the peripheral direction. The same trend as mentioned above was reported in other literatures [8]. In this analysis, however, the following new result was obtained that the unexpected high stress and strain appeared in the cladding inner surface at the position apart from the pellet's cracks.

4. Discussion

4-1 Influence of friction coefficient on the stress/strain distribution

Gittus et al. [2] proposed an expression for evaluating the concentration factor of the local strains on the basis of a membrane strain analysis [7]. They showed that the concentration factor was related to a friction coefficient, the number of cracks and a hardening coefficient of cladding material. Rand et al. [1] analysed the concentration factor by means of a plane strain problem introducing the concept of a gap element. Levy et al. [9] proposed a tri-axial PCI model in which spring and friction elements were adopted to treat the contact condition.

In the present analysis the slipping phenomenon between pellet and cladding was simulated by assumption that a fictitious thin layer existed at the interface. This assumption was reasonably accepted, because some plastic flows were observed in the thin layer of cladding inner surface after the friction test under a high contact pressure of 6 kg/mm^2 ($\sim$8500 psi) as typically shown in Photo. 1.

The result by means of the method mentioned above showed that peak height of local stress/strain became sharp as the radially cracked pellet expanded outwardly the cladding especially in the case that μ = 1.0 and 1.5. It seemed that the occurrences of the local stress/strain was not so serious problem in the case that μ = 0.5, because the peaks did not remarkably appear and also the strain concentration factor was almost constant (α = 1.5) as shown in Figs. 10 and 11. Since it can be expected that there is not very much change in the value of μ (μ = 0.5) at the initial stage of irradiation, this result might suggest that local stress/strain due to PCI at initial stage could be neglected. The stress/strain concentration factor might be useful to estimate peak stress/strain which was one of important factors for dicision of PCI induced SCC failure criterion of fuel rod. One of the significant questions to be solved will be the exact evaluation of friction coefficient between fuel pellet and cladding interface in reactor operation, since the factor is strongly influenced by the friction coefficient.

4-2 Apprication to PCI/SCC failure analysis

The cladding failures due to SCC have been observed in both PWR and BWR [10]. To prevent these failures, it has been required that reactor operating modes minimize a power ramping. PCI/SCC failure was caused when stress and strain in the cladding exceeded the fracture strength of the material which was attacked by fission products. It has been generally known that SCC failures in Zry-2 cladding occur even when the cladding stress and strain are very low [10]. This means that peak stress and strain i.e., local stress and strain caused by PCI can easily exceed a threshold stress of SCC failure. The result obtained in the present study indicated that PCI-induced SCC failure mostly occurred at the inner surface of cladding faced to pellet's cracks and might also be caused in the cladding inner surface at the position apart from the pellet's crack (see Fig. 11, (B-1) and (B-2)). The failure at the latter position may occur when the threshold stress and strain of SCC failure is very low and the friction coefficient is high.
From the result of the present analysis, it was concluded that to keep the friction coefficient as low as possible within 0.5 might be one of measures which prevent PCI-induced SCC failure.

5. Summary

The following summaries can be derived from the results obtained by the friction tests and the subsequent calculations of local stress and strain in Zry-2 cladding.

(1) The friction coefficient under a condition of hard contact is measured to be about 0.5 at temperature region of 300-400 ^{o}C.
(2) Evaluation of local stress/strain in cladding is important to predict PCI induced SCC failure especially when the friction coefficient exceeds 0.5.
(3) PCI-induced SCC failure of cladding initiates not only at the position just faced to pellet's cracks but also at the position apart from the cracks when the friction coefficient becomes larger than 1.0.

(4) Keeping the friction coefficient below 0.5 in fuel rod must be one of measures which prevent PCI induced SCC failure during reactor operation.

References

[1] for example, R. A. Rand et al., 3rd SMIRT c/2 (1975).
[2] J. H. Gittus, Nucl. Eng. Design, 18 (1972) 69.
[3] J. H. Gittus et al., Nucl. Appli. and Tech. 9 (1970) 40.
[4] O. C. Zienkiewicz and Y. K. Cheung, "The finite element method in structural and continuum mechanics", McGraw-Hill (1976).
[5] B. A. Boley and J. H. Weiner, "Theory of thermal stress", John Wiley & Sons Inc., (1960).
[6] E. Smith et al., EPRI NP-330 (1976) p.2-1.
[7] T. Udoguchi et al., Trans. Int. Conf. on Structural Mechanics in Reactor Technology c2/3 (1977).
[8] for example, E. Rolstad, Nucl. Tech. 25 (1975) 7.
[9] S. Levy and J. P. D. Wilkinson, Nucl. Eng. Design, 29 (1974) 157.
[10] for example, F. L. Yaggee et al., Trans. ANS, 30 (1978) 199.
[11] A. Pedel and D. E. Novion, J. Nucl. Mat., 33 (1969) 40.
[12] T. Udoguchi, PNC internal report, ZJ360-76-03 (1975).
[13] S. M. Lang, U. S. Nat. Bur. Standards Monograph, 6, (1960).

Table 1 Mechanical property data used in the analysis

	Zry-2 cladding	UO_2 pellet
Young's modulus		
kg/mm^2	9753.0	21000.0*
psi	1.39×10^7	3.0×10^7
Poisson's ratio	0.329**	0.300***
Yield strength		
kg/mm^2	44.0**	Assume to be not yielded
psi	6.26×10^4	
Tangent modulus		
kg/mm^2	767.0**	—
psi	1.1×10^6	
Friction coefficient between UO_2 and Zry-2.	Case 1 ; o.5 Case 2 ; 1.0 Case 3 ; 1.5	

* Reference(11), ** Reference(12), *** Reference(13)

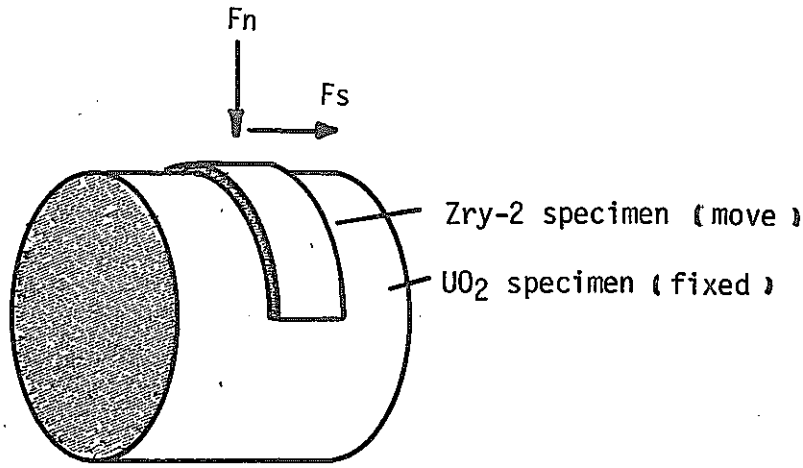

Fig.1 Scheme of the specimens for friction test.

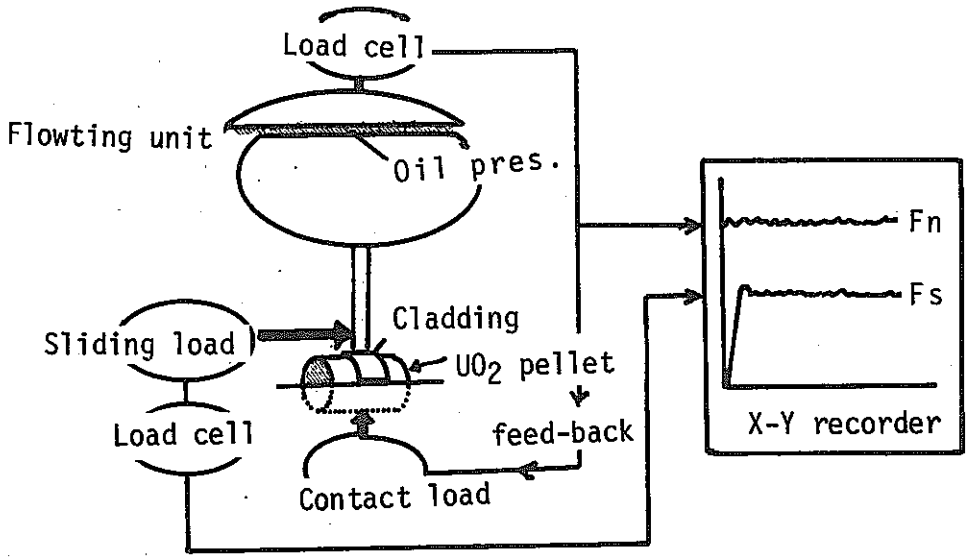

Fig.2 Schematic diagram of the testing apparatus.

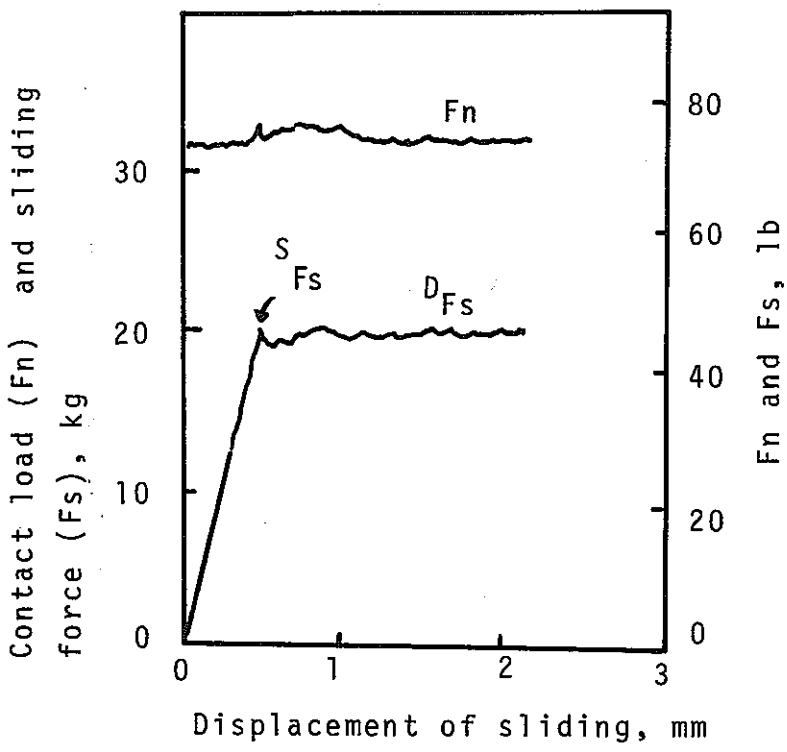

Fig.3 Typical relation between load and displacement.

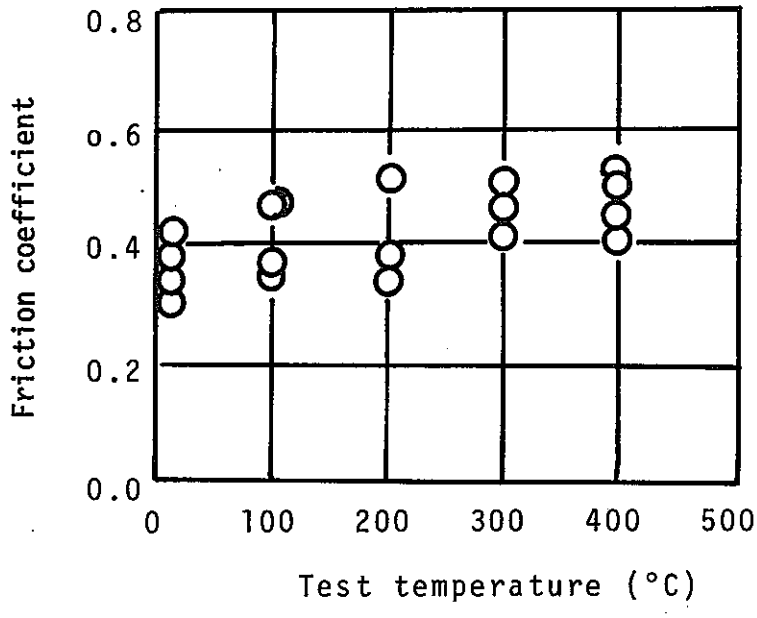

Fig.4 Friction coefficients of UO_2/Zry-2 as a function of test temperatures.

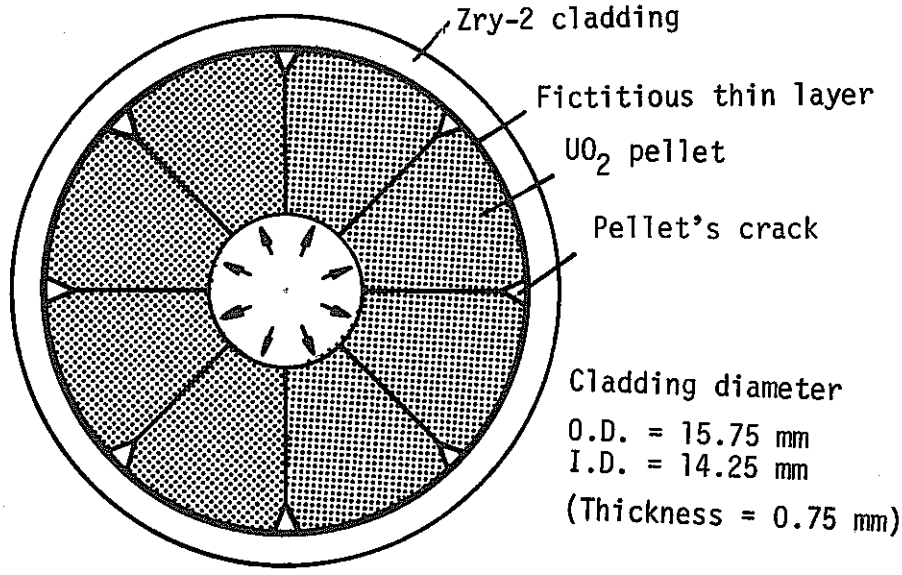

Fig.5 Model used PCI analysis

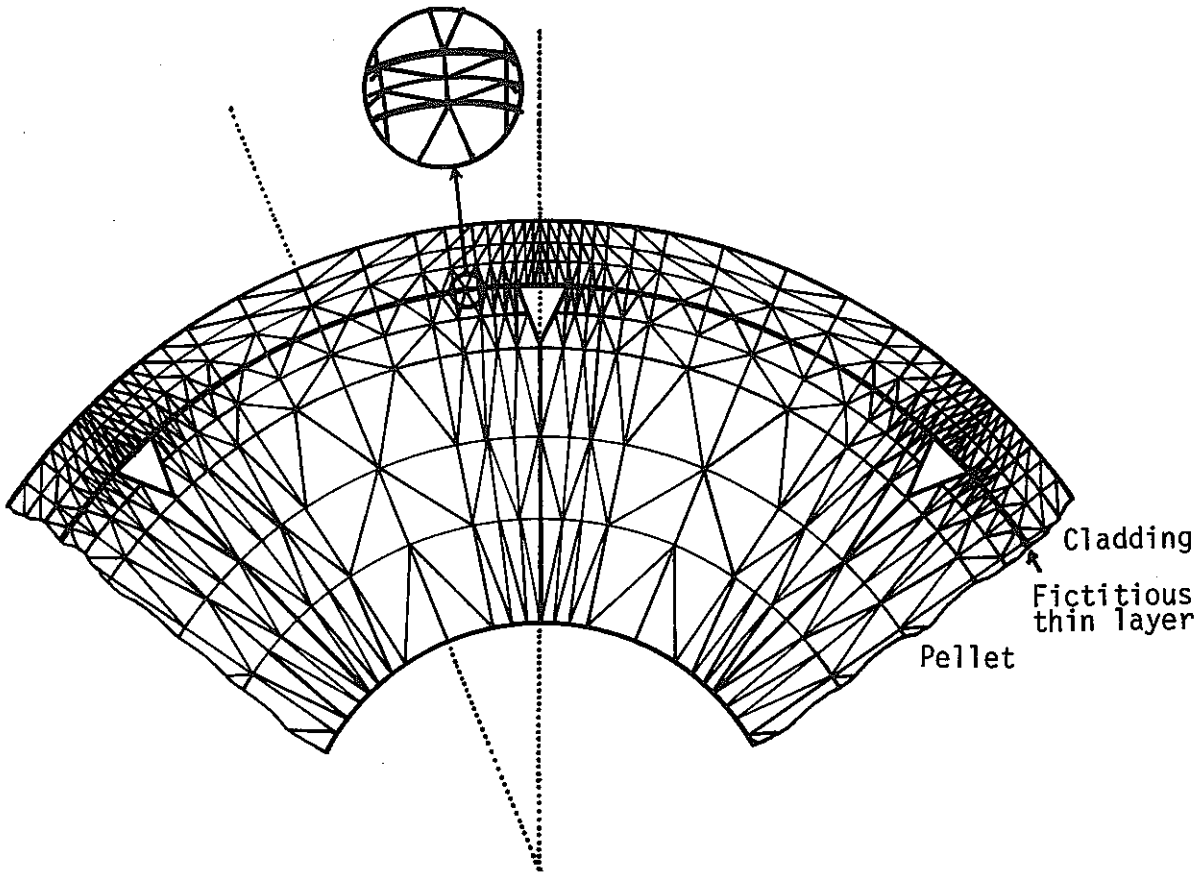

Fig.6 Finite element layout

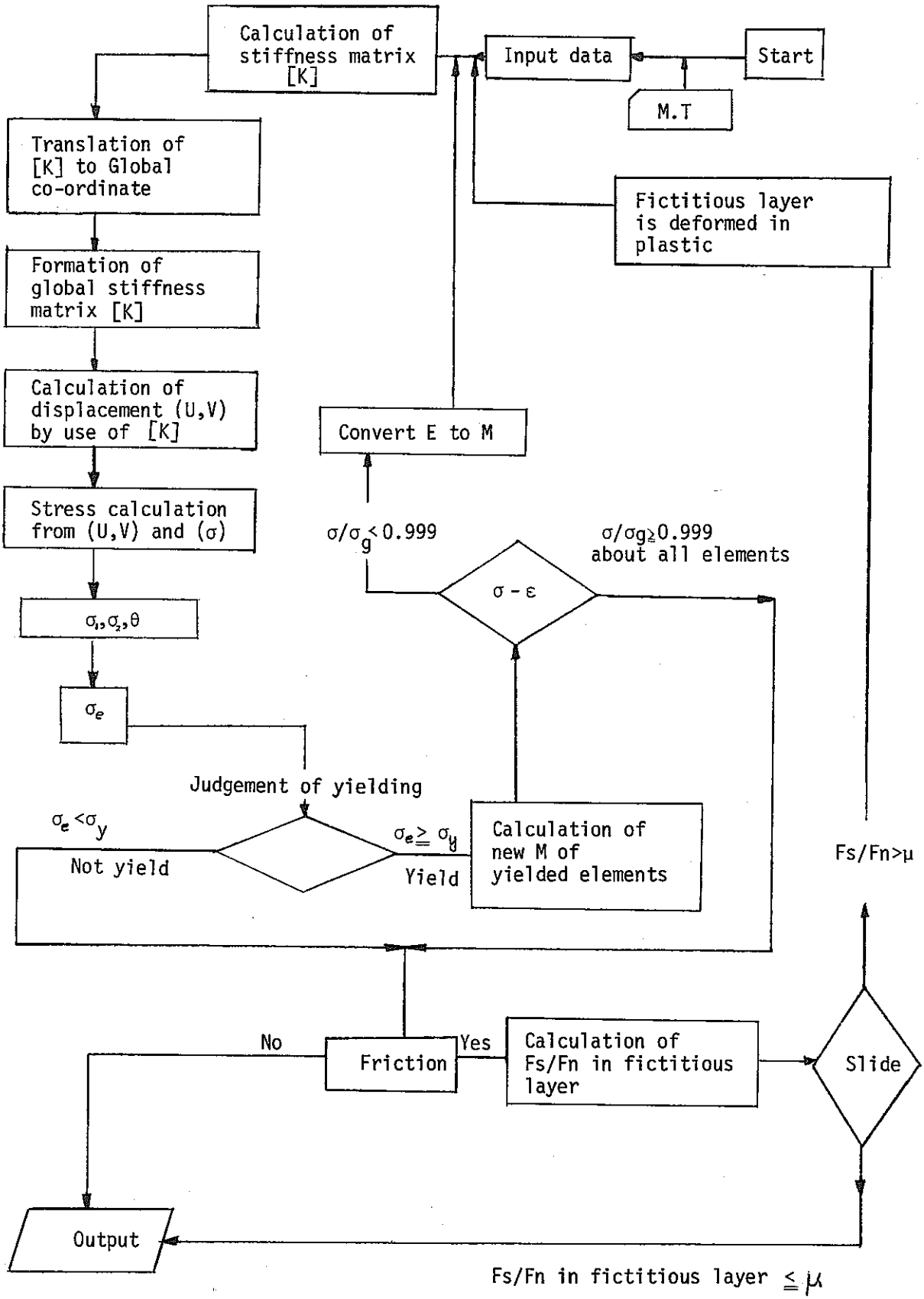

Fig. 7 Flow diagram for "PLASTIC" code.

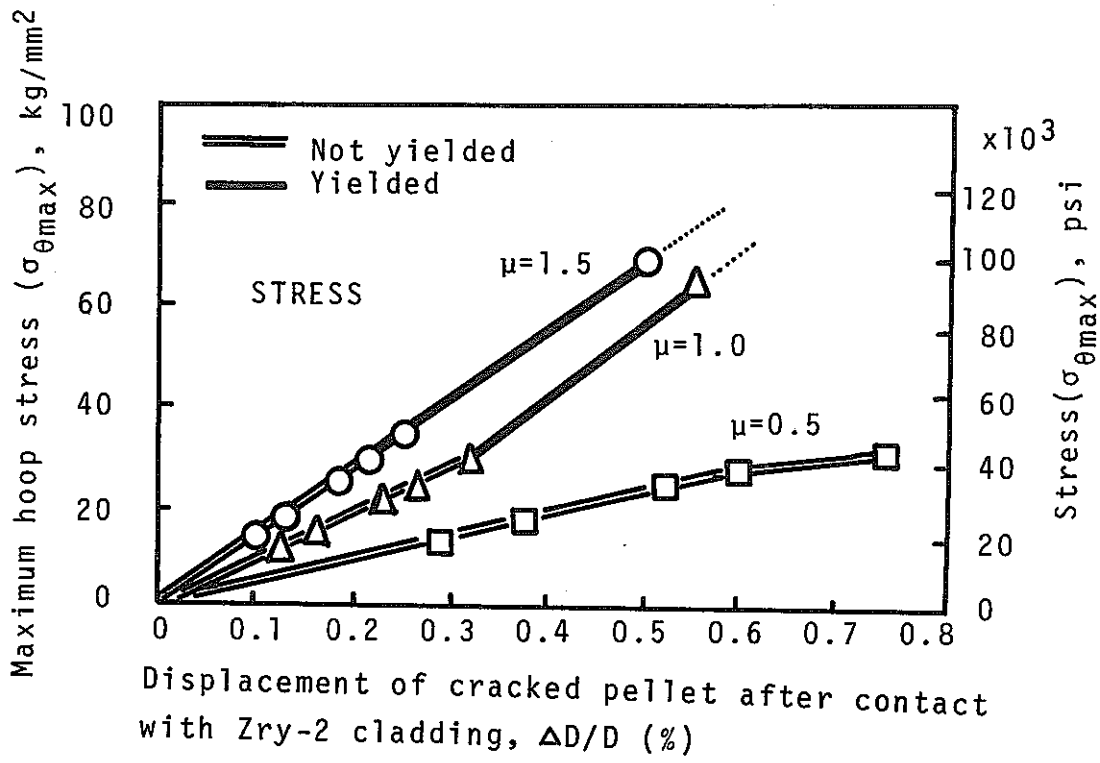

Fig.8 Change of the maximum hoop stress in Zry-2 cladding due to the expansion of cracked pellet

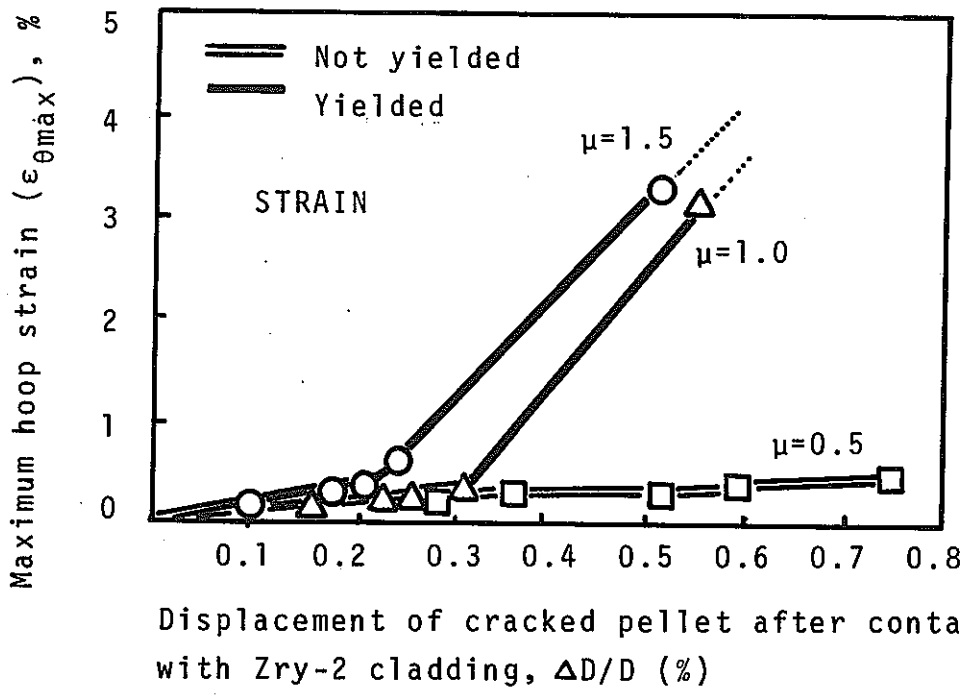

Fig.9 Change of the maximum hoop strain in Zry-2 cladding due to the expansion of cracked pellet.

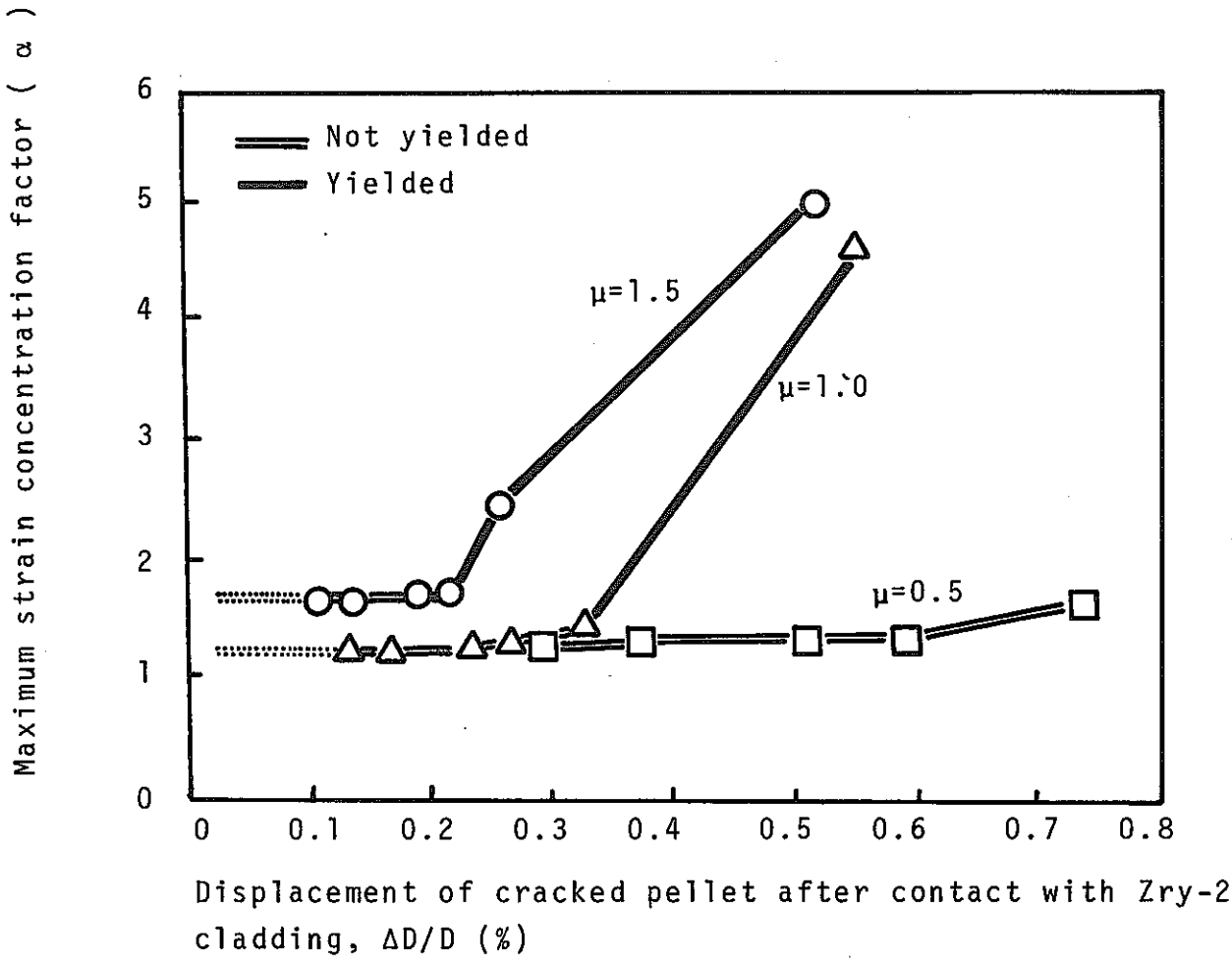

Fig.10 Change of the maximum strain concentration factors in Zry-2 cladding due to the expansion of cracked pellet.

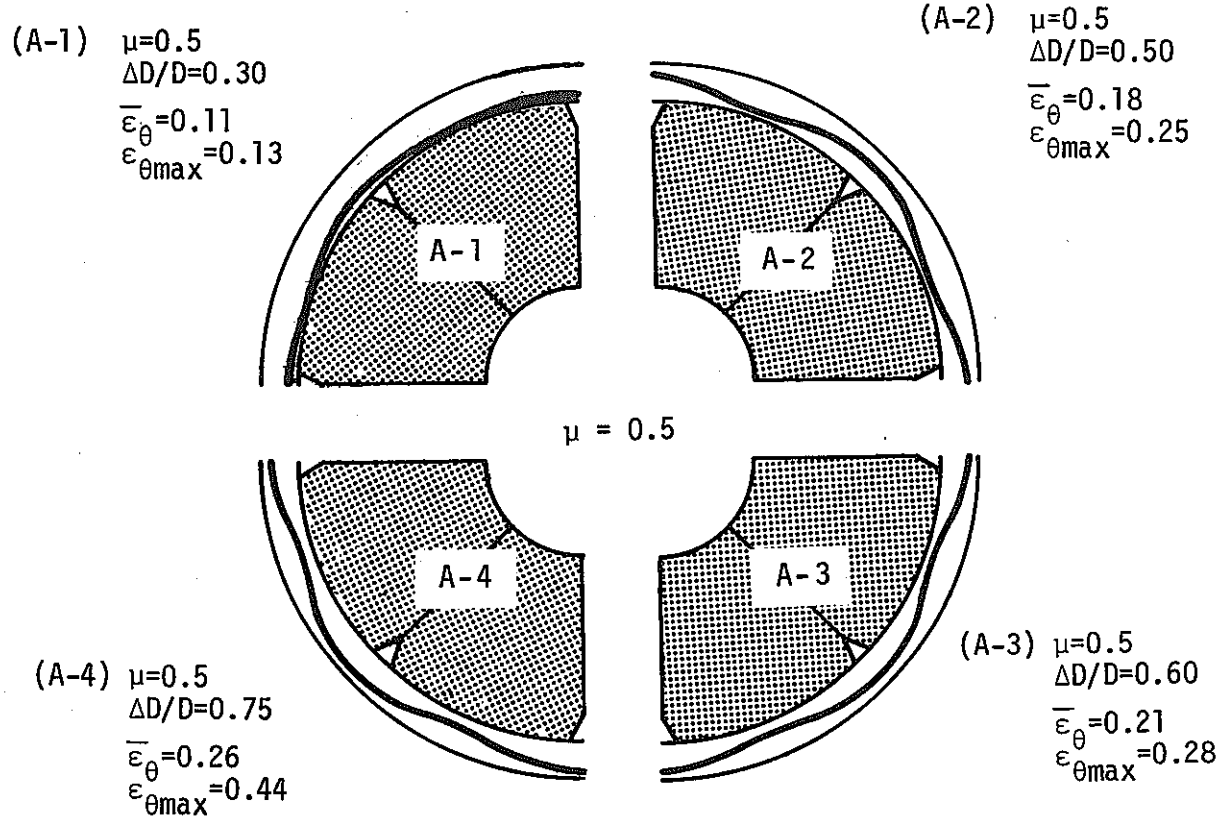

Fig.11 (A) Calculation results of hoop strain distributions at inner surface of Zry-2 cladding by expansion of cracked pellet.

μ	: Friction coefficient
ΔD/D(%)	: Displacement of cracked pellet after contact with the cladding
$\overline{\varepsilon}_\theta$	: Mean tensile hoop strain
$\varepsilon_{\theta max}$	: Maximum tensile hoop strain

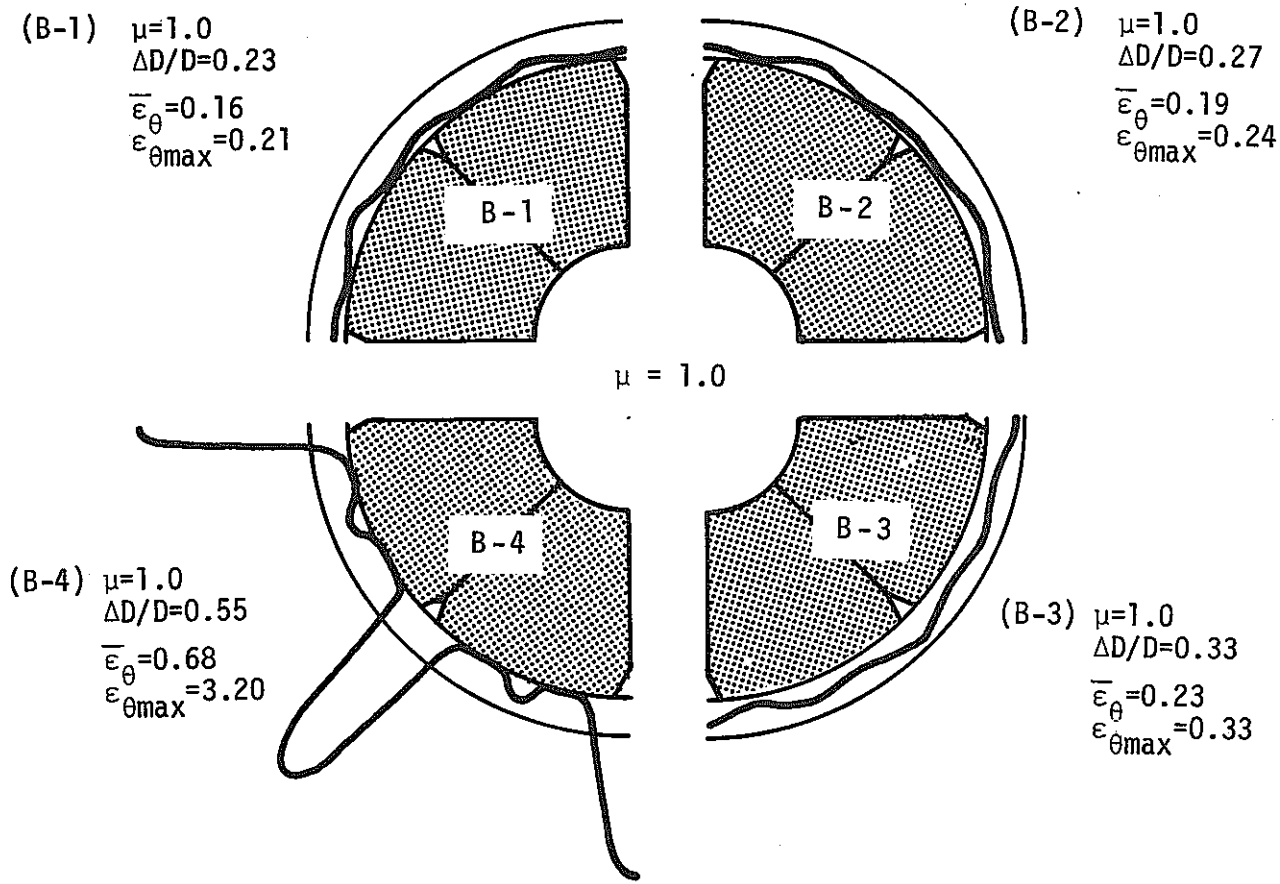

Fig.11 (B) Calculation results of hoop strain distributions at inner surface of Zry-2 cladding by expansion of cracked pellet.

μ	: Friction coefficient
ΔD/D(%)	: Displacement of cracked pellet after contact with the cladding
$\overline{\varepsilon}_\theta$	: Mean tensile hoop strain
$\varepsilon_{\theta max}$	: Maximum tensile hoop strain

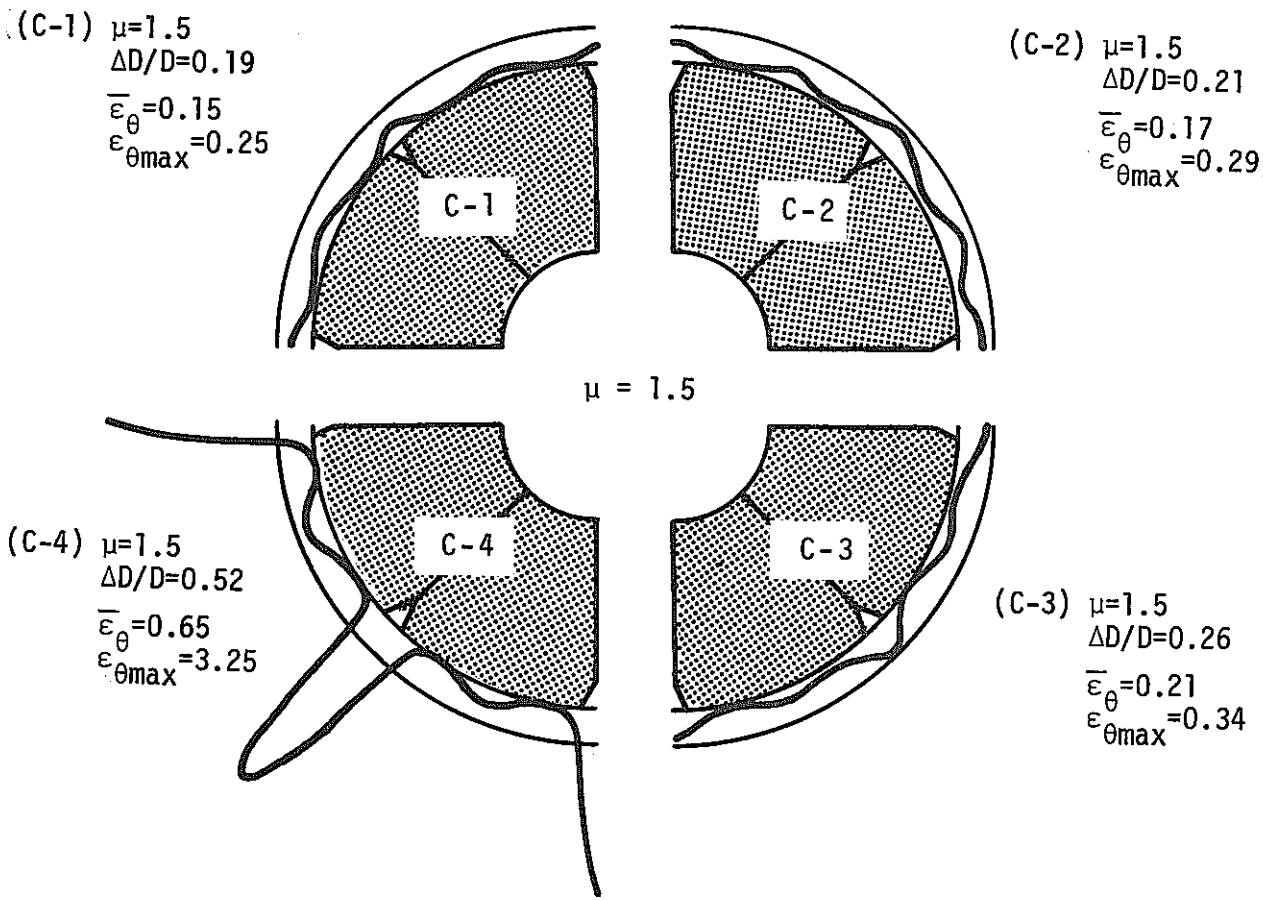

Fig.11 (C) Calculation results of hoop strain distributions at inner surface of Zry-2 cladding by expansion of cracked pellet.

μ	: Friction coefficient
ΔD/D(%)	: Displacement of cracked pellet after contact with the cladding
$\overline{\varepsilon}_\theta$	: Mean tensile hoop strain
$\varepsilon_{\theta max}$	: Maximum tensile hoop strain

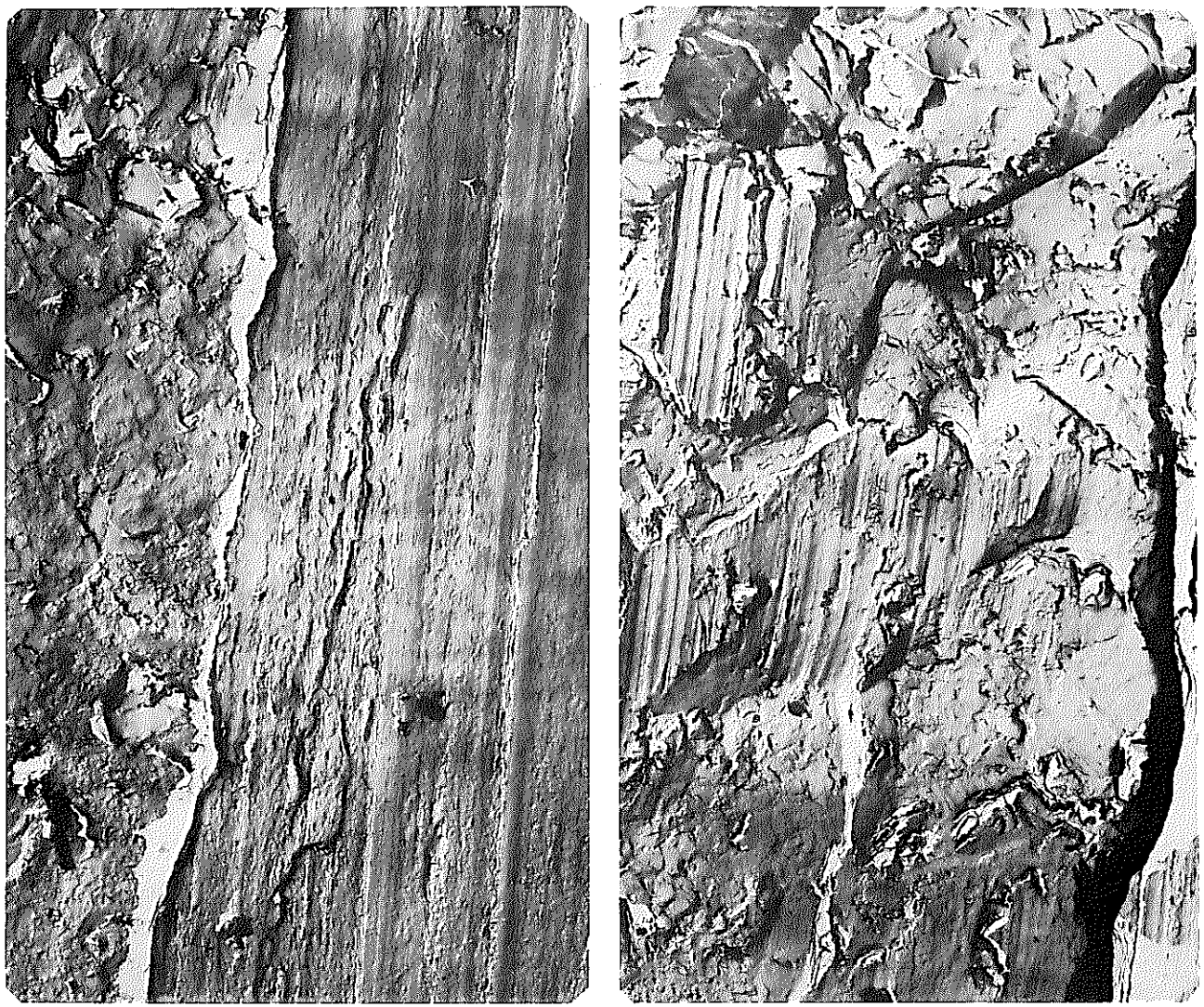

AFTER SLIDE TESTING AT 400°C

2. μ

Photo.1 ELECTRON MICROGRAPHS (ZRY-2)